Photoinduced Processes in Some Mechanically Interlocked Supramolecules as Studied by Time-Resolved Electron Paramagnetic Resonance

ARTICLE *in* THE JOURNAL OF PHYSICAL CHEMISTRY C · NOVEMBER 2011

Impact Factor: 4.77 · DOI: 10.1021/jp2073655

5 AUTHORS, INCLUDING:

Alexander Berg
Hebrew University of Jerusalem
20 PUBLICATIONS **375** CITATIONS

SEE PROFILE

David I Schuster
New York University
247 PUBLICATIONS **5,739** CITATIONS

SEE PROFILE

Photoinduced Processes in Some Mechanically Interlocked Supramolecules as Studied by TREPR

Journal:	*The Journal of Physical Chemistry*
Manuscript ID:	Draft
Manuscript Type:	Article
Date Submitted by the Author:	n/a

Complete List of Authors:	Jakob, Manuela; Hebrew University of Jerusalem, Physical Chemistry Berg, Alexander; Hebrew University of Jerusalem, Physical Chemistry Levanon, Haim; Hebrew University of Jerusalem, Physical Chemistry Schuster, David; New York University, Chemistry Megiatto Jr, Jackson; Arizona State University

Photoinduced Processes in Some Mechanically Interlocked Supramolecules as Studied by TREPR

Manuela Jakob,[§] Alexander Berg,[§] Haim Levanon,[§] David I. Schuster[‡] and Jackson D. Megiatto, Jr.[‡ζ]*

[§]Department of Physical Chemistry, Hebrew University of Jerusalem, Jerusalem 91904, Israel

[‡]Department of Chemistry, New York University, New York, NY 10003, USA

[ζ]Present address: Department of Chemistry and Biochemistry, Arizona State University, Tempe, AZ 85287, USA

*E-mail: levanon@chem.ch.huji.ac.il

RECEIVED DATE (to be automatically inserted after your manuscript is accepted if required according to the journal that you are submitting your paper to)

Abstract Time-resolved electron paramagnetic resonance (TREPR) spectroscopy was used for studying photoinduced intramolecular electron transfer (ET) and energy transfer (EnT) processes in three mechanically interlocked molecules in which zinc(II)porphyrin (ZnP) and C_{60} fullerene moieties are arrayed around a central Cu(I) bisphenanthroline core used to assemble these donor-acceptor (D-A) systems. The specific molecules studied include a "long" $(ZnP)_2$-Cu(I)$(phen)_2$-C_{60} rotaxane as well as ZnP-Cu(I)$(phen)_2$ and ZnP-Cu(I)$(phen)_2$-C_{60} catenanes, embedded in different phases of nematic liquid crystal and frozen isotropic solvents. It was demonstrated that the routes and rates of the transfer processes in these supramolecules strongly depend on the characteristics of their microenvironment and the molecular entity which was selectively photoexcited. This is reflected by formation of distinct long-lived charge-separated species such as the radical ion pair $(ZnP)_2^{\cdot+}$-Cu(I)$(phen)_2^{\cdot-}$ and the metal-to-ligand charge-separated state Cu(II)-$(phen)_2^{\cdot-}$ under the various experimental conditions. The results are discussed in terms of the correlation between the chemical structure, conformational mobility, and relaxation pathways of the photoexcited states in these mechanically interlocked systems. Results are compared with previously reported TREPR data on related interlocked D-A porphyrin/fullerene systems.

KEYWORDS: Rotaxanes**,** Catenanes, Photoexcited states, Photoinduced electron and energy transfer, Time-resolved EPR

Introduction Light-driven electron and energy transfer processes are the key steps in natural photosynthesis, and elucidating their mechanisms continues to attract considerable interest in different disciplines.[1-3] The complexity of the *in vivo* photosynthetic apparatus has prompted the search for the relatively simple artificial model systems that can mimic processes and states occurring under natural solar energy conversion and storage.[4-9,10,11] It is well established that the chromophores in the natural reaction centers are highly organized by the protein matrix in which the systems are embedded, providing optimal topography for fast and efficient photoinduced intra- and intermolecular energy transfer (EnT) and electron transfer (ET) processes and significantly slower back electron transfer (BET). Still, many aspects of such structural organization remain poorly understood, and a diversity of artificial donor-acceptor (D-A) systems are subjects of extensive investigation.[5,8,12] In this context, supramolecules such as rotaxanes and catenanes in which D and A moieties are mechanically interlocked rather than covalently linked seem to be particularly promising biomimetic systems.[13,14] A detailed understanding of structure-function relationships in mechanically interlocked D-A supramolecules which takes solute-solvent interaction into consideration is also necessary for designing novel "smart" nanodevices such as molecular machines and molecular motors.[15-19]

Topologically, catenanes consist of two or more interlocked rings, while rotaxanes possess a ring threaded on a rod bearing terminal bulky substituents to prevent dissociation.[19-22] Catenates are catenanes containing a central metal core, such as Cu(I). These arrays possess much higher mobility of their component moieties as compared to that in more conventional covalently linked arrays. In addition to the rotational and vibrational motions possible in chemically bonded ensembles, the mechanically interlocked entities are capable of performing translational movements relative to each other.[23] Hence, flexible rotaxanes as well as more structurally rigid catenanes could serve as building blocks for materials and devices whose properties can be manipulated by external stimuli. In photoactive rotaxanes and catenanes, light absorption induces conformational changes that in turn affect mutual arrangement of the supramolecular moieties, thus modifying intramolecular ET and EnT routes and rates.[17,23-29] It is noteworthy that among the systems with such architectures, porphyrin-fullerene

arrays are particularly attractive due to the remarkable properties of porphyrins as electron donors[26,30] and of fullerenes as electron acceptors.[31-33]

We have recently reported on the photophysical properties of a group of rotaxanes assembled using Sauvage's metal templating strategy,[16,34,35] containing free base or zinc(II) porphyrin electron donor groups as end groups on the rod and C_{60} fullerene acceptor moieties on the macrocycle, mechanically linked through a central Cu(I)bisphenanthroline (Cu(I)$phen_2$) complex.[36,37] Reference rotaxanes lacking the C_{60} moiety were also investigated. In both these systems the Cu(I)$(phen)_2$ complex after visible light absorption gives rise to the excited singlet and triplet metal-to-ligand charge transfer states (MLCT) states, which can act as the efficient mediator or acceptor of energy or an electron.[38,39] We demonstrated in our earlier work[36,37] that the efficiencies and pathways of light-driven ET and EnT processes in $(ZnP)_2$-Cu(I)$(phen)_2$, $(ZnP)_2$-Cu(I)$(phen)_2$-C_{60}, $(H_2P)_2$-Cu(I)$(phen)_2$ and $(H_2P)_2$-Cu(I)$(phen)_2$-C_{60} rotaxanes strongly depend on the properties of their microenvironment, as reflected by formation of distinct charge separated states under different experimental conditions.[36,37]

We now extend our studies to include a newly synthesized "long" $(ZnP)_2$-Cu(I)$(phen)_2$-C_{60} rotaxane, where the linkage between ZnP and the Cu(I)$(phen)_2$ is lengthened by triazole groups,[40] and two topologically distinct [2]catenates, namely ZnP-Cu(I)$(phen)_2$ and ZnP-Cu(I)$(phen)_2$-C_{60},[41] in order to gain deeper insight into the correlation between structure and function in these topologically distinct nanoscale supramolecular arrays (for structures, see Figure 1).

The experimental method employed in this study is X-band (9.5 GHz) time-resolved electron paramagnetic resonance (TREPR) combined with selective laser light excitation of the supramolecular moieties. The measurements were performed in frozen isotropic solvents and in different phases of the nematic liquid crystal (LC) E-7. High sensitivity, spectral and time resolution of EPR spectroscopy, together with the use of magnetically oriented LC as a solvent, enable following of transient paramagnetic species in the system of interest in real time. Analysis of the TREPR spectra under different experimental conditions provides additional information not derivable from optical studies about dynamic, kinetic, and magnetic parameters associated with the ET precursors and intermediates.

Thus, the experimental data obtained over a wide range of solvents, temperatures, and time intervals successfully complements information achieved in optical spectroscopy for revealing the mechanisms associated with ET and EnT processes.[42-46]

Experimental Toluene (A. C. S. Reagent, J. T. Baker Inc.) was dried and kept under vacuum during sample preparation. Ethanol (Chromasolv, Absolute, HPLC grade, Sigma-Aldrich), tetrahydrofuran (THF) (A. C. S. Reagent, Merck Ltd.), and LC (E-7, Merck Ltd.) were used without further purification. The phase transitions of the solvents are given below:

$$\begin{aligned}
&\text{E-7:} && \textit{crystalline} \xleftrightarrow{210\,\text{K}} \textit{soft crystalline} \xleftrightarrow{263\,\text{K}} \textit{nematic} \xleftrightarrow{333\,\text{K}} \textit{isotropic} \\
&\text{Toluene:} && \textit{glass} \xleftrightarrow{117\,\text{K}} \textit{amorphous} \xleftrightarrow{178\,\text{K}} \textit{liquid} \qquad \textbf{(1)} \\
&\text{Ethanol:} && \textit{glass} \xleftrightarrow{97\text{K}} \textit{amorphous} \xleftrightarrow{156\,\text{K}} \textit{liquid} \\
&\text{THF:} && \textit{glass} \xleftrightarrow{164.5\text{K}} \textit{liquid}
\end{aligned}$$

Procedures for synthesis of the compounds used in this study, which are present as PF_6^- salts, are described elsewhere.[40,41,47] The compounds were first dissolved in toluene (~ 5 x 10^{-4} M), which was then evaporated and the LC was introduced into the Pyrex tube. The samples were degassed by several freeze-pump-thaw cycles on a vacuum line and sealed under vacuum.

X-band TREPR experiments (response time 150-200 ns) were performed in degassed 4 mm O.D. Pyrex tubes employing a Bruker ESP 380 EPR spectrometer with field modulation disconnected.[48] The EPR signals were taken from the microwave preamplifier and transferred to a Le Croy LT 262 digital oscilloscope after being passed through a low–noise filter and amplified by a fast amplifier (10 dB). A frequency counter (EIP, Model 545) was used to monitor the microwave frequency. Estimation of the g-factors was performed employing magnetic field and microwave frequency controllers, namely a precision NMR Teslameter PT 2025 (Metrolab), and microwave frequency counter EIP 545, respectively. Transient traces of the EPR signals were acquired and accumulated on a PC through a GPIB interface. The spectra at different time windows after the laser pulse were reconstructed from the full set of data obtained over a chosen scan range of the magnetic field. The temperature was controlled

by a Bruker variable temperature unit (Model ER411 VT). The samples were illuminated by an optical parametric oscillator (OPO) (Panther III, Continuum Corp.) pumped by the third harmonic (355 nm) of a Nd:Yag laser (Surelite II, Continuum Corp.) with 7-10 mJ/pulse OPO output, 10 Hz repetition rate and 10 ns pulse duration.

The orientation of the LC director, **L**, with respect to the magnetic field, **B**, is determined by the sign of the anisotropy of the diamagnetic susceptibility, $\Delta\chi$ ($\Delta\chi = \chi_{\parallel} - \chi_{\perp}$).[49] Since $\Delta\chi$ is positive for E-7, the default orientation in the nematic phase is **L** ∥ **B**. Rotation of the frozen sample by 90° about an axis perpendicular to the external magnetic field yields the director orientation **L** ⊥ **B**. Analysis of the TREPR line shapes was performed as described elsewhere.[50,51] The radical pair (RP) spectra were analyzed in terms of spin correlated radical pair (SCRP) and triplet radical pair (TRP) mechanisms.[52-54] In all EPR experiments, the spectra did not show any saturation effects over the wide microwave power range (15 - 93 mW) and the corresponding kinetics did not exhibit any oscillations, satisfying underdamping conditions.[55]

The intramolecular distances between the photoactive moieties (ZnP, C_{60} and $Cu(I)(phen)_2$) were calculated employing HyperChem modeling, which allows computing the minimal energy molecular geometry in its ground state in vacuum. Thus, in condensed media the computed spacing between the rotaxane component entities should be regarded as best estimates due to possible conformational changes.

Results and Discussion

We first present the main photophysical parameters of the three D-A systems studied here (Figure 1). Since the quenching routes of the photoexcited states of the chromophore depend on their microenvironment,[56] For TREPR experiments isotropic solvents of different polarity (toluene, dielectric constant $\varepsilon = 2.38$[57], tetrahydrofuran (THF) $\varepsilon = 7.52$[57], ethanol, $\varepsilon = 25.3$[57]) and anisotropic LC E-7 ($\varepsilon_{\parallel} = 19.0$, $\varepsilon_{\perp} = 6.2$)[58] were used over a wide range of temperatures corresponding to the different states of these media. Samples were excited selectively at either 460 or 532 nm. At 460 nm the absorption of the $Cu(I)(phen)_2$ moiety is maximal ($\kappa \approx 1700$ cm^{-1} M^{-1})[59] while the absorption of ZnP is minimal ($\kappa \approx 1550$

$cm^{-1} M^{-1}$).[60] On the other hand, at 532 nm, $Cu(I)(phen)_2$ absorption is low ($\kappa \approx 270$ $cm^{-1} M^{-1}$), while ZnP absorption is high ($\kappa \approx 8150$ $cm^{-1} M^{-1}$).[60] The extinction coefficients of C_{60} at 460 and 532 nm are 200 $cm^{-1} M^{-1}$ and 840 $cm^{-1} M^{-1}$, respectively.[61] Thus, the probabilities of 460 nm light absorption by the $(ZnP)_2$, $Cu(I)(phen)_2$ and C_{60} entities in the compounds of interest correspond roughly to the ratio of their extinction coefficients, namely 1.8:1:0.1 at 460 nm, and 60:1:3 at 532 nm for the "long" rotaxane **1a** and 0.9:1:0.1 at 460 nm, and 30:1:3 at 532 nm for the catenate **1c**. Therefore, upon 460 nm excitation, [2]catenate **1b** with–photoexcited ZnP and $Cu(phen)_2$ entities should be formed with comparable probabilities, while on excitation at 532 nm, the photoexcited ZnP moiety will dominate. In the case of "long" rotaxane **1a**, ZnP and $Cu(phen)_2$ electronic excited states will both be generated upon irradiation of **1a** at 460 nm, prevailing over excited C_{60}, while most of the photons at 532 nm will be predominantly absorbed by ZnP and to a lesser extent by C_{60} as compared to $Cu(I)(phen)_2$.

The excited singlet and triplet states energies of the photoactive moieties in **1a-1c** are as follows: ZnP: 2.12 and 1.59 eV;[62] $Cu(I)(phen)_2$: 1.91 and 1.73 eV (averaged);[63,64] and C_{60}: 1.80 and 1.57 eV, respectively.[62] The extinction coefficients and excited state energies are taken as those for the pristine compounds, namely Zn(II)tetraphenylporphine ZnTPP, pseudorotaxane $Cu(I)(phen)_2$ and C_{60}. We assume that the values of these parameters for the moieties in the mechanically interlocked supramolecular systems are approximately the same as those of the corresponding pristine compounds. It is worth noting that all of the above state energies were determined in liquid isotropic solvents and may change slightly under our experimental conditions, so they are only estimates. Unfortunately, corresponding precise values in the frozen isotropic solvents and LC matrices are not available.

$(ZnP)_2$-Cu(I)$(phen)_2$-C_{60} rotaxane 1a

Isotropic solvents

TREPR spectra of **1a** obtained after photoexcitation at both 460 and 532 nm in toluene consist of two overlapping signals: a broad a/e signal of ~70 mT width and a superimposed narrow signal of peak-to-peak value ΔH_{pp} ~ 5.9 mT (Figure 2). Based on the similarity of the signal parameters with those

found for photoexcited pristine ZnTPP[65,66] and C_{60}[67,68] under similar experimental conditions, we attribute them to the lowest triplet states of the ZnP and C_{60} rotaxane entities, respectively. Unfortunately, TREPR experiments on **1a** could not be performed in ethanol because of its very low solubility in this solvent.

Anisotropic solvents

Photoexcitation of the rotaxane in the crystalline phase of the LC at 460 and 532 nm at both L||B and L⊥B sample orientations gives rise to TREPR spectra consisting of three signals (Figure 3). Analysis of the two a/e signals with ~ 70 mT width and ΔH_{pp} ~7.7 mT allowed assignment of them to the lowest triplet states of ZnP and C_{60} rotaxane moieties, respectively. Spectral characteristics of these signals are very similar to those of pristine ZnTPP[65,66] and C_{60},[67,68] observed under the same experimental conditions. A third signal, which exhibits e/a polarization pattern and ~ 45 mT width was observed after 460 nm excitation (Figure 3 c). Inspection of Figure 3 shows that this additional signal is especially pronounced at L||B orientation. This same signal but with a lower signal-to-noise ratio is also observed at 460 nm excitation in the soft crystalline phase of E-7 at 240K where only L||B orientation of LC can be achieved (not shown). It should be emphasized here that the spectral parameters of this signal are very different from those typically seen for ZnP[65,66] and C_{60}.[67,68] It is noteworthy that a very similar signal was also observed on photoexcitation of the (ZnP)-Cu(I)$(phen)_2$ [2]catenate (see below). Speculation as to the origin of this spectral feature is deferred to a later section.

It was found that the TREPR spectra taken upon 532 nm excitation in both crystalline and soft crystalline phases of the LC are practically identical, but possess lower signal to noise ratio compared with the spectra observed after 460 nm excitation.

(ZnP)-Cu(I)$(phen)_2$ [2]catenate 1b

Isotropic solvents

Since [2]catenate **1b** is poorly soluble in toluene, we used THF as an isotropic solvent where the solubility was good. Photoexcitation of **1b** at both 460 and 532 nm light gives rise to similar TREPR

spectra of ~70 mT width and a/e polarization pattern. Figure 4 presents the spectra observed in frozen THF at 460 and 532 nm excitation. The similarity of the parameters of these spectra with the spectrum of pristine ZnTPP allows assignment of this signal to the lowest triplet state of the ZnP moiety. The slight distortion of the ZnP triplet spectrum observed at 460 nm excitation could be the result of EnT from ^{3}MLCT* to ^{3}ZnP*.[69] We believe that this EnT process is much more efficient on excitation at 460 nm, where the extinction coefficients of ZnP and Cu(I)(phen)$_2$ are similar, rather than at 532 nm where the ratio of these coefficients is 30:1.

Anisotropic solvent

Excitation of **1b** at 460 nm in the crystalline phase of LC E-7 at the L||B orientation gives rise to three overlapping signals: (a) a wide (~70 mT) a/e signal with a low signal to noise ratio, (b) a narrower e/a signal of 45 mT width, and (c) an even narrower a/e signal with a g ~ 2.00 and ΔH_{pp} ~1.1 mT (Figure 5). The widest signal is attributed to the triplet state of ZnP because it exhibits very similar parameters to the spectrum of ZnTPP.[65,66] The narrower 45 mT e/a signal is akin to the additional signal observed in the case of the "long" (ZnP)$_2$-Cu(I)(phen)$_2$-C$_{60}$ rotaxane **1a** (see above) under the same experimental conditions (Figure 3). The narrowest signal is assigned to a charge separated state, the origin of which will be discussed later.

The spectrum obtained upon 460 nm excitation of **1b** at L⊥B orientation in E-7 also comprises three very similar signals: (a) wide a/e of ~70mT width, (b) narrower e/a ~45 mT width and (c) a very narrow a/e signal with ΔH_{pp} ~1.2 mT (Figure 5).

In the soft crystalline phase of LC, TREPR spectra (Figure 6) exhibit only two signals: the wide e/a signal of ~ 45 mT width and the a/e signal with ΔH_{pp} ~1.2 mT peak to peak distance which is attributed to the charge separated (CS) state. The origin of both signals will be discussed below. It should be noted that the polarization patterns of all these signals do not change with time.

Photoexcitation of [2]catenate **1b** at 532 nm in E-7 at 170 K gives rise to the broad spectrum assigned to ^{3}ZnP*, while at 240 K the spectrum exhibits only an e/a signal of ~45 mT width. The spectra of **1b** upon 532 nm excitation possess a low signal-to-noise ratio and are not shown. It should be noted

that the e/a signal of ~45 mT is similar to those detected in spectra of rotaxane **1a** (Figure 3) as well as [2]catenate **1b** after 460 nm excitation (Figures 5 and 6). The possible origin of this signal will be discussed in a later section.

Under conditions with impeded diffusion, i. e., in frozen and viscous matrices, two pathways leading to charge-separated (CS) state formation can account for the observed multiplet radical pair (RP) signal, namely triplet radical pair (TRP) and weakly coupled spin-correlated radical pair (SCRP) mechanisms. Well elaborated theory of these mechanisms allows us to draw conclusions about a precursor to and mechanism of the RP formation and identification of its participants. It was found that the polarization patterns of these signals are the same at both **L** ∥ **B** and **L** ⊥ **B** orientations and do not change in time. The finding that the RP signal phase does not depend on the sample orientation relative to the external magnetic field, points to the mechanism of RP formation. Specifically, for weakly coupled SCRP with small values of ZFS parameter D and exchange interaction J, the phase of the signal should depend on the molecular orientation of the RP with respect to the magnetic field[53,70] according to the following equation:

$$Dzz = D(3\cos^2\xi - 1) \qquad (\mathbf{2})$$

where D is the dipolar interaction and ξ is the angle between the RP dipolar axis and the magnetic field direction. Taking into account that $J \rightarrow 0$ in a weakly coupled SCRP, one can conclude that in such pairs the dominant interaction between the constituents is angle-dependent dipolar coupling.[53] Thus, phase inversion of the RP spectrum upon sample rotation in the solid phase of the LC, is predicted from eq 2 when the dipolar angle ξ is replaced by $(\xi + 90^\circ)$.[71,72] Thus, rotation of the sample by 90° should result in inversion of the RP signal (from e/a to a/e), in contrast to the observed signal phase behavior.

On the other hand, for a strongly coupled TRP mechanism, the RP phase should remain unchanged at **L** ∥ **B** and **L** ⊥ **B** orientations, as is the case.[53] Therefore, the observed narrow signal for **1b** is assigned to the TRP formed by intramolecular ET between the $^1ZnP^*$ and the $Cu(I)(phen)_2$ entities in the [2]catenate. We previously showed that formation of the [$ZnP^{\bullet-}$-$Cu(II)(phen)_2$] and [$ZnP^{\bullet+}$-

$Cu(0)(phen)_2$] radical pairs can be ruled out on thermodynamic grounds.[34,35,73] Thus, by default, we suggest that the [$ZnP^{\bullet+}$-$Cu(I)(phen)_2^{\bullet-}$] charge-separated radical pair (CSRP) state is responsible for the narrowest signal. This suggestion is in line with the signal parameters. First of all, the g value of ~2.00 for the signal is close to that of the theoretically predicted TRP signal, which should be centered about the mean value (g ~ 2.0024) of the g-factors of the RP's constituents, namely $ZnP^{\bullet+}$ with g ~ 2.0025[74], and $Cu(I)(phen)_2^{\bullet-}$ with g ~ 2.0023. The g value of the latter species is assumed to be close to that of a typical organic radical, given that the influence of Cu(I) should be minor because of localization of the transferred electron in the MLCT state on the ligand.[75] The linewidth of this narrow signal of only ~1.2 mT supports our suggestion. HyperChem modeling indicates the distance between the centers of ZnP and $Cu(I)(phen)_2$ is 20 Å (Figure 7) At this distance both dipolar and exchange interactions between the electrons are operative and contribute to the linewidth. The point dipole approximation, given by the equation:

$$|D| = 3/4[(g\beta)^2/r^3] \quad (\mathbf{3})$$

with a g-factor of 2.00, β = Bohr magneton, and r = 20 Å, gives a value of 0.35 mT for the width ΔH_{pp} ($\Delta H_{pp} \sim D$) of the narrow signal assigned to the TRP. Furthermore, at such distances the *J*-value is expected to be only a few mT.[76] Since the *D* parameter of such a RP is usually negative, one can assume that for the observed RP width of ~1.2 mT the *J* value must possess a positive sign.[77-79]

Based on the arguments presented above, we propose the mechanism shown in Figure 8 for charge-separated state formation in $(ZnP)_2$-$Cu(I)(phen)_2$ [2]catenate **1b**. Photoexcitation of the $Cu(I)(phen)_2$ moiety forms the MLCT state, ([$Cu(II)(phen)_2^{\bullet-}$]), where the electron is mostly localized on the ligand.[36,37,75] In this MLCT state Cu(II) is a powerful oxidant, capable of oxidizing the ZnP moiety even in its ground state,[80] similar to the reaction found in related MLCT systems.[36,37,81] As a result, the CSRP state [$(ZnP)_2^{\bullet+}$ - $Cu(I)(phen)_2^{\bullet-}$] is formed, which is responsible for the observed narrow signal observed for [2]catenate **1b**.

(ZnP)-Cu(I)(phen)$_2$-C$_{60}$ [2]catenate 1c

Isotropic solvents

The low solubility of **1c** in glass-forming solvents, such as toluene, ethanol, and *o*-dichlorobenzene, did not allow us to carry out experiments in an isotropic microenvironment.

Anisotropic solvents

Photoexcitation of **1c** at both 460 and 532 nm at 170 K in the crystalline phase of LC at L⊥B orientation results in practically identical TREPR spectra comprising two overlapping signals: (a) a wide a/e signal of ~ 68 mT width, and (b) a superimposed narrow a/e signal of ΔH_{pp} ~ 8.3 mT width (see Figure 9). These parameters are similar to those of photoexcited pristine ZnTPP[65,66] and C$_{60}$[67,68] under similar experimental conditions, allowing assignment of them to the lowest triplet states of the ZnP and C$_{60}$ moieties, respectively.

The signals for [2]catenate **1c** at L||B orientation in E-7 possess a much lower signal-to-noise ratio and are not shown. In the soft crystalline phase of LC the spectra of **1c** exhibit only one signal with a low signal-to-noise ratio, which we attribute to the lowest triplet state of C$_{60}$[67,68] (not shown). No evidence suggestive of formation of a charge-separated (CS) state was found in the case of catenate **1c** in the LC medium at low temperatures.

As suggested earlier,[41] [2]catenate **1c** adopts an extended conformation with the chromophores as far as possible from each other. Despite this, formation of the CS state (ZnP)$^{\cdot+}$-Cu(I)(phen)$_2$-C$_{60}^{\cdot-}$ was detected by fast optical spectroscopy in liquid isotropic solvents at ambient temperatures. The absence of noticeable ET from ZnP to C$_{60}$ in [2]catenate **1c** at low temperatures under our experimental conditions can be explained by the large distance between the D and A moieties in **1c** (Figure 10) as compared to the D-A distances in previously studied (ZnP)$_2$-Cu(I)(phen)$_2$-C$_{60}$ and (H$_2$P)$_2$-Cu(I)(phen)$_2$-C$_{60}$ rotaxanes.[36,37] The more rigid catenane structure also hampers conformational tuning of the ET efficiency, especially in very viscous LC media at low temperatures (170-240 K).

Comparison of the results presented in this paper with the optical and TREPR spectroscopic data gained earlier[36,37,40,41,82] shows that the relaxation of the photoexcited states in these mechanically interlocked ensembles occurs differently in glassy, amorphous, and liquid states of isotropic solvents as well as in the crystalline and nematic phases of LC. We attribute these findings to the capability of the rotaxanes and catenanes to perform considerable conformational changes depending on the parameters of the microenvironment and the temperature. In turn, these molecular modifications combined with the variation in the solvent properties may have a noticeable effect on the observed relaxation pathways and dynamics of the electronic excited states of these interlocked D-A systems.

The additional signal observed in the spectra of 1a and 1b

Practically identical broad (~45 mT) signals were observed for the photoexcited "long" $(ZnP)_2$-Cu(I)$(phen)_2$-C_{60} rotaxane **1a** and the (ZnP)-Cu(I)$(phen)_2$ [2]catenate **1b**, but not for the (ZnP)-Cu(I)$(phen)_2$-C_{60} [2]catenate **1c**.

First, let us consider the simpler (ZnP)-Cu(I)$(phen)_2$ [2]catenate **1b.** Inspection of Figure 5 shows that together with two weak signals, which were attributed to the triplet states of ZnP and RP, an additional intense e/a signal of 45 mT width is also observed. The lowest triplet state of ZnP, which gives an a/e spectrum of 70 mT width, cannot account for this signal. This is true as well for the spectrum of the ZnP triplet, which could be formed after charge recombination of the RP. Furthermore, we can not attribute this signal to a distorted spectrum of the ZnP triplet, formed as result of the triplet-triplet energy transfer from the MLCT triplet state.[69] Even assuming that the observed inversion of the spectral polarization pattern as compared to the "pure" ZnP triplet spectrum is a result of such distortion, it could not account for a signal linewidth as large as 45 mT.

Since a practically identical signal was also observed in the TREPR spectra of the $(ZnP)_2$-Cu(I)$(phen)_2$-C_{60} rotaxane **1a**, as shown in Figure 3, the 45 mT signal is not attributable to C_{60}. In any case, the lowest triplet state of C_{60} is characterized by an a/e spectrum with significantly narrower width.[67,68]

The 45 mT signal also cannot be ascribed to the polarized doublet ground state of the Cu(II) moiety, which would result in a net absorption or emission signal,[83] but not the observed e/a signal. This signal is also not attributable to the triplet state of phenanthroline, since this state can only be created by using significantly shorter wavelength irradiation, ~390 nm vs 460 and 532 nm used in our experiments. Such a species would exhibit significantly larger spectral width (~200 mT vs ~45 mT).[84]

Based on these arguments, we suggest by default that the species responsible for the 45 mT signal is the MLCT triplet state of Cu(II)(phen)$_2$. Unfortunately, overlapping of the spectra of the various moieties in these compounds (namely ZnP and MLCT triplets in catenate **1b** and ZnP, C_{60} and MLCT triplets in the rotaxane **1a**) did not allow us to separate out the undistorted spectrum of MLCT triplets in order to perform computer simulations to determine its ZFS and triplet sublevels population parameters. Attempts to make experiments on the separate Cu(II)(phen)$_2$ pseudorotaxane (with unfunctionalized tails) failed because of its very poor solubility in glass-forming solvents such as toluene and ethanol.

We need to address the reasons why the MLCT triplet spectrum was detected in the case of the (ZnP)$_2$-Cu(I)(phen)$_2$-C_{60}–rotaxane **1a** and (ZnP)-Cu(I)(phen)$_2$ [2]catenate **1b** but was absent in the spectrum of (ZnP)-Cu(I)(phen)$_2$-C_{60} [2]catenate **1c**. First, let us consider excitation of the simpler [2]catenate **1b** at 460 nm, where the numbers of molecules with photoexcited porphyrin and fullerene moieties are expected to be similar (see above). For catenate **1b** signals for ^{3}ZnP*, ^{3}MLCT* and weak RP spectra were observed in LC, while a distorted ^{3}ZnP* signal was observed in an isotropic solvent. Thus, in the case of catenate **1b** in LC medium at low temperatures, RP formation is apparently not efficient. Thus, only small fractions of the electronically excited ZnP and MLCT states seem to be engaged in the ET process under these conditions. As a result, the spectrum of catenate **1b** in the LC medium exhibits signals for ^{3}ZnP*, ^{3}MLCT* and weak RP signals. On the other hand, upon excitation of **1b** in an isotropic solvent, ^{3}MLCT* is quenched by fast EnT to generate the ZnP triplet, and as a result we observe only signals for the distorted ^{3}ZnP* state. The LC possesses very different parameters as compared to the isotropic solvents. As discussed previously,[36,37] the variation in the solvent properties

strongly affects the thermodynamic parameters of the relevant reactions, which in turn significantly modifies the rates and routes of the ET and EnT processes occurring upon electronic excitation. For catenate **1b** excited at 532 nm, the ratio of extinction coefficients of the ZnP and $Cu(I)(phen)_2$ moieties is now 30:1. Under conditions where EnT from ZnP to $Cu(I)(phen)_2$ is efficient (soft crystalline phase of LC, 240 K), we observe a signal for the $^3MLCT^*$ state, while in the crystalline LC phase (170 K) and in frozen isotropic solvent, the EnT process apparently does not occur, resulting in observation of only a $^3ZnP^*$ signal. We propose that changes in the catenane conformation occurring in LC could facilitate EnT from the $^1ZnP^*$ to give singlet and/or triplet MLCT states.

On the other hand, in rotaxane **1a**, the large separation between D and A moieties, as obtained from HyperChem modeling (Figure 11), significantly impedes ET and EnT processes. Thus, we believe that in LC media upon 460 nm excitation, the $^3MLCT^*$ is efficiently generated, but is not quenched by subsequent ET and EnT events, which makes its detection possible. When this rotaxane is irradiated at 532 nm, where the extinction coefficient of the $Cu(I)(phen)_2$ is low, too few of the MLCT states are created to allow its observation in our experimental setup.

Optical studies of **1a** in isotropic solvent at room temperature showed that under these conditions, a series of ET and EnT processes occur to generate a long- lived (400 – 500 ns in various solvents) charge-separated state in which an electron has been transferred from the ZnP to the C_{60} moiety.[85] It is noteworthy that this intermediate is not observed in the TREPR experiments, either in LC or in isotropic media.

Here, we should note that molecular modeling, using both Spartan with PM3 minimization[40,41] and HyperChem programs, provided practically identical conformations for [2]catenates **1b** and **1c**, while the calculated conformations for the rotaxane **1a** were noticeably different. More specifically, in the extended conformation of **1a,** as obntained from HyperChem both ZnP moieties are separated from the fullerene by the same distance of 23 Å (Figure 11). On the other hand, in the bent conformation of **1a**, obtained from Spartan`s PM3 modeling,[40,41] one ZnP is close to the fullerene while the other ZnP is more distant (4 and 24 Å, respectively).[85] As mentioned above, both programs generate the most stable

molecular conformation in vacuum at room temperature. Of course, there is no way of knowing what precise conformation rotaxane **1a** adopts at ambient or low temperatures in its excited states in either the LC or isotropic media.

The absence of noticeable charge separation in the case of the extended conformation of **1a** is explained above in terms of large distance between D and A which reduces efficiencies of the ET processes. Considering the bent conformation of rotaxane **1a**, we can explain the absence of signals for the CSRP state in our TREPR experiments on rotaxane **1a** as follows. In **1a**, the distance between the far ZnP and C_{60} moieties is too large for efficient ET, while the RP formed as a result of ET from the close ZnP to C_{60} should possess too short a lifetime to be detected in our experimental setup. Moreover, even if such long-lived charge-separated state was generated under our experimental conditions, we would not expect to observe its signal because of a significant broadening caused not only by dipole-dipole interactions (eq 2) but also by exchange interactions, which are very powerful at such short distances.[76]

We should note here that for previously studied $(ZnP)_2$-Cu(I)$(phen)_2$ and $(ZnP)_2$-Cu(I)$(phen)_2$-C_{60} as well as for $(H_2P)_2$-Cu(I)$(phen)_2$ and $(H_2P)_2$-Cu(I)$(phen)_2$-C_{60} rotaxanes[36,37] the $^3MLCT^*$ state was not detected under any experimental conditions. For free base rotaxanes, computer analysis of the $^3H_2P^*$ and $^3MLCT^*$ signals shows that even if the latter were present, it would be completely masked by the H_2P triplet spectrum. On the other hand, efficiently formed long-lived $^3MLCT^*$ states obtained upon photoexcitation of the ZnP rotaxanes ought to be detectable in principle. Thus, their absence in the spectra of these rotaxanes[36,37] implies that either it was formed in small amounts or, if formed, it was rapidly quenched by various ET and/or EnT processes occurring subsequently in these systems.

Summary.

It is demonstrated that photoinduced processes in the $(ZnP)_2$-Cu(I)$(phen)_2$-C_{60} rotaxane **1a** as well as in the (ZnP)-Cu(I)$(phen)_2$ and (ZnP) -Cu(I)$(phen)_2$-C_{60} [2]catenates **1b** and **1c** are different in the disparate media. Specifically, the rates and efficiencies of ET and EnT reactions in these

mechanically interlocked macromolecules depend significantly on their microenvironment. Analysis of the results obtained in this study together with those gained recently for $(ZnP)_2$-Cu(I)$(phen)_2$-C_{60}, $(ZnP)_2$-Cu(I)$(phen)_2$, $(H_2P)_2$-Cu(I)$(phen)_2$-C_{60}, and $(H_2P)_2$-Cu(I)$(phen)_2$ rotaxanes[36,37] lead us to the following conclusions. We believe that the high conformational mobility of these supramolecules, particularly in the rotaxanes, allows modification of electronic coupling between donor and acceptor entities due to solute-solvent interactions, affecting parameters of the light-induced processes. This is attributable to the ability of the mechanically interlocked supramolecules to change not only the mutual orientation of the donor and acceptor moieties as compared with conventional covalently linked structures, but also the distance between these molecular entities by various external stimuli. This is confirmed by molecular modeling, which showed that even in the ground state of the supramolecules in vacuum, the mutual arrangement of their entities differs dramatically, for example upon changing the porphyrin core or attaching the fullerene moiety.[36,37,40,41,85] Almost surely such phenomena will occur also for the electronically excited supramolecules upon changing their microenvironment.

We believe that understanding the structure-function-medium relationships in rotaxanes and catenanes will open new horizons for designing novel "smart" molecular systems with controllable properties for further application in different fields of science and technology.

Acknowledgments. The work at HUJ was supported by Deutsche Forschungsgemeinschaft (Grant HE 5206/2-1), and the KAMEA foundation (A. B.). This work is in the fulfillment of the requirements for a Ph.D. degree (M.J.) at HUJ. Support of the work at NYU by a grant from the National Science Foundation (CHE-0647334) is acknowledged with grateful appreciation.

Figure Captions

Figure 1. The structures of (a) "long" $(ZnP)_2$-Cu(I)$(phen)_2$-C_{60} rotaxane, (b) (ZnP)-Cu(I)$(phen)_2$ [2]catenate, and (c) (ZnP)-Cu(I)$(phen)_2$-C_{60} [2]catenate.

Figure 2. TREPR spectrum of the rotaxane **1a** in frozen toluene (140K) at 532 nm excitation, 940 ns after the laser pulse.

Figure 3. TREPR spectra of rotaxane **1a** in E-7 at 170 K at L∥B (a,c) and at L⊥B (b,d) orientations. Spectra a and b were recorded 850 ns after laser pulse photoexcitation at 532 nm. Spectra c and d were recorded 950 ns after laser pulse photoexcitation at 460 nm. The arrows in c indicate the features of the additional signal.

Figure 4. TREPR spectra of [2]catenate **1b** in frozen THF (150K) at (a) 532 nm excitation, 900 ns after the laser pulse and (b) 460 nm excitation, 1060 ns after the laser pulse.

Figure 5. TREPR spectra of [2]catenate **1b** in E-7 at 170 K at (a) L∥B and (b) at L⊥B orientations. Spectra were recorded 940 ns (a) and 900 ns (b) after the laser pulse of 460 nm. RP signals are enclosed in the circles.

Figure 6. TREPR spectrum of [2]catenate **1b** in the soft crystalline phase of E-7 (240K) at 460 nm excitation, 1300 ns after the laser pulse. The RP signal is enclosed in a circle.

Figure 7. HyperChem structure of [2]catenate **1b**.

Figure 8. General presentation of the possible photoinduced processes occurring in [2]catenate **1b** in E-7, where L = $(phen)_2$.

Figure 9. TREPR spectrum of [2]catenate **1c** in E-7 at 170 K at L⊥B orientation, at 532 nm photoexcitation, 900 ns after laser pulse.

Figure 10. HyperChem structure of [2]catenate **1c**.

Figure 11. HyperChem structure of rotaxane **1a**.

References

(1) Noy, D. *Photosynt. Res.* **2008**, *95*, 23.

(2) Nocera, D. G. *Inorg. Chem.* **2009**, *48*, 10001.

(3) Renger, G. *Curr. Sci.* **2010**, *98*, 1305.

(4) Benniston, A. C.; Harriman, A. *Materials Today* **2008**, *11*, 26.

(5) Gust, D.; Moore, T. A.; Moore, A. L. *Acc. Chem. Res.* **2009**, *12*, 1890.

(6) Ricks, A. B.; Solomon, G. C.; Colvin, M. T.; Scott, A. M.; Chen, K.; Ratner, M. A.; Wasielewski, M. R. *J. Am. Chem. Soc.* **2010**, *132*, 15427.

(7) Gagliardi, C. J.; Westlake, B. C.; Kent, C. A.; Paul, J. J.; Papanikolas, J. M.; Meyer, T. J. *Coord. Chem. Rev.* **2010**, *254*, 2459.

(8) Gray, H. B.; Winkler, J. R. *BBA-Bioenergetics* **2010**, *1797*.

(9) Taniguchi, M.; Lindsey, J. S. *Tetrahedron* **2010**, *66*, 5549.

(10) Albinsson, B.; Martensson, J. *Phys. Chem. Chem. Phys.* **2010**, *12*, 7338.

(11) Kalyanasundaram, M. G. *Current Opinion in Biotechnology* **2010**, *21*, 298.

(12) McConnell, I.; Li, G.; Brudvig, G. W. *Chem. & Biol.* **2010**, *17*, 434.

(13) Duerr, H.; Bossmann, S. *Acc. Chem. Res.* **2001**, *34*, 905.

(14) Sauvage, J. P.; Collin, J., P.; Faiz, J. A.; Frey, J.; Heitz, V.; Tock, C. *J. Porphyrins Phthalocyanines* **2008**, *12*, 881.

(15) Benniston, A. C.; Harriman, A. *Angew. Chem. Int. Ed.* **1993**, *32*, 1459.

(16) Sauvage, J.-P. *Acc. Chem. Res.* **1998**, *31*, 611

(17) Brouwer, A. M.; Fazio, S. M.; Frochot, C.; Gatti, F. G.; Leigh, D. A.; Wong, J. K. Y.; Wurpel, G. W. H. *Pure Appl. Chem.* **2003**, *75*, 1055.

(18) Willner, I.; Basnar, B.; Willner, B. *Adv. Funct. Mater.* **2007**, *17*, 702.

(19) Stoddart, J. F. *Chem. Soc. Rev.* **2009**, *38*, 1802.

(20) Bravo, J. A.; Raymo, F. M.; Stoddart, J. F.; White, A. J. P.; Williams, D. J. *Eur. J. Org. Chem.* **1998**, 2565.

(21) Kay, E. Rotaxanes and Catenanes. The University of Edinburgh. Available at http://www.catenane.net/home/rotcatintro.html (accessed August 2011).

(22) *Molecular Catenanes, Rotaxanes and Knots: A Journey Through the World of Molecular Topology*; Sauvage, J.-P.; Dietrich-Buchecker, C., Ed.; Wiley-VCH: Weinheim, 1999.

(23) Mateo-Alonso, A.; Ehli, C.; Rahman, G. M. A.; Guldi, D. M.; Fioravanti, G.; Marcaccio, M.; Paolucci, F.; Prato, M. *Angew. Chem. Int. Ed.* **2007**, *46*, 3521.

(24) Stowell, M. H. B.; McPhillips, T. M. *Science* **1997**, *276*, 812.

(25) Darrouzet, E.; Valkova-Valchanova, M.; Moser, C. C.; Dutton, P. L.; Daldal, F. *Proc. Natl. Acad. Sci.* **2000**, *97*, 4567.

(26) El-Khouly, M. E.; Ito, O.; Smith, P. M.; D'Souza, F. *J. Photochem. Photobiol. C-Photochem. Rev.* **2004**, *5*, 79.

(27) Sandanayaka, A. S. D.; Watanabe, N.; Ikeshita, K. I.; Araki, Y.; Kihara, N.; Furusho, Y.; Ito, O.; Takata, T. *J. Phys .Chem. B* **2005**, *109*, 2516.

(28) Balzani, V.; Credi, A.; Venturi, M. *Chem. Soc. Rev.* **2009**, *38*, 1542.

(29) Megiatto, J. D. J.; Schuster, D. I. Interlocked Artificial Photosynthetic Model Systems Composed of Electron Donor and [60]Fullerene Units. In *Fullerenes: Principles and Applications*; 2 ed.; Langa, F., Nierengarten, J. F., Eds.; The Royal Society of Chemistry.: Cambridge, 2011; pp 354.

(30) Jurow, M.; Schuckman, A. E.; Batteas, J. D.; Drain, C. M. *Coord. Chem. Rev.* **2010**, *254*, 2297.

(31) Ohkubo, K.; Fukuzumi, S. *J. Porphyrins Phthalocyanines* **2008**, *12*, 993.

(32) Balzani, V.; Credi, A.; Venturi, M. *Chem. Sus. Chem.* **2008**, *1*, 26.

(33) Seitz, W.; Kahnt, A.; Guldi, D. M.; Torres, T. *J. Porphyrins Phthalocyanines* **2009**, *13*, 1034.

(34) Sauvage, J.-P. *Acc. Chem. Res.* **1990**, *23*, 319.

(35) Linke, M.; Chambron, J.-C.; Heitz, V.; Sauvage, J.-P. *J. Am. Chem. Soc* **1997**, *119*, 11329.

(36) Jakob, E.; Berg, A.; Rubin, R.; Levanon, H.; Li, K.; Schuster, D. I. *J. Phys .Chem. A* **2009**, *113*, 5846.

(37) Jakob, M.; Berg, A.; Levanon, H.; Schuster, D. I.; Megiatto, J. D. J. *J. Phys. Chem. A* **2011**, *115*, 5044.

(38) Flamigni, L.; Armaroli, N.; Barigelletti, F.; Chambron, J.-C.; Sauvage, J.-P.; Solladie, N. *New J. Chem.* **1999**, *23*, 1151.

(39) Lockard, J. V.; Kabehie, S.; Zink, J. I.; Smolentsev, G.; Soldatov, A.; Chen, L. X. *J. Phys. Chem. B* **2010**, *114*, 14521.

(40) Megiatto, J. D. J.; Spencer, R.; Schuster, D. I. *Org. Lett.* **2009**, *11*, 4152.

(41) Megiatto, J. D. J.; Schuster, D. I.; Abwandner, S.; de Miguel, G.; Guldi, D. *J. Am. Chem. Soc.* **2010**, *132*, 3847.

(42) Levanon, H.; Hasharoni, K. *Prog. React. Kinet.* **1995**, *20*, 309.

(43) Levanon, H. *Adv. Photosynth.* **1996**, *3*, 211.

(44) Savitsky, A.; Möbius, K. *Photosynt. Res.* **2009**, *102*, 311.

(45) Allen, J. P.; Cordova, J. M.; Jolley, C. C.; Murray, T. A.; Schneider, J. W.; Woodbury, N. W.; Williams, J. C.; Niklas, J.; Klihm, G.; Reus, M.; Lubitz, W. *Photosynt. Res.* **2009**, *99*, 1.

(46) Ponomarenko, N. S.; Poluektov, O. G.; Bylina, E. J.; Norris, J. R. *BBA-Bioenergetics* **2010**, *1797*, 1617.

(47) Megiatto, J. D. J.; Schuster, D. I. Synthesis of Electron Donor-[60]Fullerene Multi-Ring Interlocked Systems. In *Handbook of Carbon Nano Materials.*; D'Souza, F., Kadish, K. M., Eds.; World Scientific: Singapore, 2011; Vol. 1: Synthesis and Supramolecular Systems.; pp 207.

(48) Jakob, M.; Berg, A.; Stavitski, E.; Chernick, E. T.; Weiss, E. A.; Wasielewski, M. R.; Levanon, H. *Chem. Phys.* **2006**, *324*, 63.

(49) Regev, A.; Galili, T.; Levanon, H. *J. Chem. Phys.* **1991**, *95*, 7907.

(50) Gonen, O.; Levanon, H. *J. Phys. Chem.* **1984**, *88*, 4223.

(51) Blank, A.; Levanon, H. *Conc. Magn. Reson. A* **2005**, *25A*, 18.

(52) Salikhov, K. M.; Molin, Y. N.; Sagdeev, R. Z.; Buchachenko, A. L. *Spin Polarization and Magnetic Effects in Radical Reactions*; Elsevier: Amsterdam, 1984.

(53) Hore, P. J. Analysis of Polarized EPR Spectra. In *Advanced EPR: Applications in Biology and Biochemistry*; Hoff, A. J., Ed.; Elsevier: Amsterdam, 1989; pp 405.

(54) Norris, J. R.; Morris, A. L.; Thurnauer, M. C.; Tang, J. *J. Chem. Phys.* **1990**, *92*, 4239.

(55) Furrer, R.; Fujara, F.; Lange, C.; Stehlik, D.; Vieth, H. M.; Vollmann, W. *Chem. Phys. Lett.* **1980**, *75*, 332.

(56) Kavarnos, G. J. *Fundamentals of Photoinduced Electron Transfer*; VCH Publishers, Inc: New York, 1993.

(57) Bialkowski, S. E. Parameters for Common Solvents Used in Photothermal and Photoacoustic Spectrometry. Utah State University, Logan, UT; Available at http://www.chem.usu.edu/~sbialkow/Research/Tablevalues.html (accessed August 2011)

(58) Merck, E. *Merck Ltd. Catalog: Nematic Liquid Crystal Mixtures*, **1989**.

(59) Ruthkosky, M.; Kelly, C. A.; Castellano, F. N.; Meyer, G. J. *Coord. Chem. Rev.* **1998**, *171*, 309.

(60) Optical Spectra; Oregon Medical Laser Center, Portland, OR; Available at http://omlc.ogi.edu/spectra/PhotochemCAD/html/ZnTPP.html (accessed August 2011).

(61) Moravsky, A. P.; Fursikov, P. V.; Kachapina, L. M.; Khramov, A. V.; Kiryakov, N. V. UV-VIS Photometric Analysis of Fullerenes C60 and C70 in Toluene and Hexane Solutions. In *Recent Advances in the Chemistry and Physics of Fullerenes*; K.M.Kadish, R. S. Ruoff, Eds.; The Electrochemical Society Inc.: Pennington,NJ, 1995; Vol. 2; pp 156.

(62) Galili, T.; Regev, A.; Levanon, H.; Schuster, D. I.; Guldi, D. M. *J. Phys. Chem. A* **2004**, *108*, 10632.

(63) Parker, W. L.; Crosby, G. A. *J. Phys .Chem.* **1989**, *93*, 5692

(64) Kirchhoff, J. R.; Gamache, R. E.; Blaskie, M. W.; Del Paggio, A. A.; Lengel, R. K.; McMillin, D. R. *Inorg. Chem.* **1983**, *22*, 2380.

(65) Gonen, O.; Levanon, H. *J. Phys. Chem.* **1985**, *89*, 1637.

(66) Scherz, A.; Levanon, H. *J. Phys. Chem.* **1980**, *84*, 324.

(67) Levanon, H.; Meiklyar, V.; Michaeli, A.; Michaeli, S.; Regev, A. *J. Phys. Chem.* **1992**, *96*, 6128.

(68) Regev, A.; Gamliel, D.; Meiklyar, V.; Michaeli, S.; Levanon, H. *J. Phys. Chem.* **1993**, *97*, 3671.

(69) Levanon, H.; Norris, J. R. *Chem. Rev.* **1978**, *78*, 185.

(70) Closs, G. L.; Forbes, M. D. E.; Norris, J. R. *J. Phys. Chem.* **1987**, *91*, 3592.

(71) Hasharoni, K.; Levanon, H.; Greenfield, S. R.; Gosztola, D. J.; Svec, W. A.; Wasielewski, M. R. *J. Am. Chem. Soc.* **1996**, *118*, 10228.

(72) Berg, A.; Shuali, Z.; Asano-Someda, M.; Levanon, H.; Fuhs, M.; Möbius, K.; Wang, R.; Sessler, J. L. *J. Am. Chem. Soc.* **1999**, *121*, 7433.

(73) Li, K.; Schuster, D. I.; Guldi, D.; Herranz, M. A.; Echegoyen, L. *J. Am. Chem. Soc.* **2004**, *126*, 3388.

(74) Felton, R. H. Redox Reactions of Metalloporphyrins. In *The Porphyrins*; Dolphin, D., Ed.; Academic Press: New York, 1978; Vol. 5; pp 53.

(75) Gordon, K. C. J.; McGarvey, J. J. *Inorg. Chem.* **1991**, *30*, 2986.

(76) Molin, Y. N.; Salikhov, K. M.; Zamaraev, K. I. *Spin Exchange, Principles and Applications in Chemistry and Biology*; Springer: New York, **1980**.

(77) Okamura, M. Y.; Isaacson, R. A.; Feher, G. *Biochim. Biophys. Acta.* **1979**, *546*, 394.

(78) Hoffmann, S. K.; Hilczer, W.; Goslar.J. *Appl. Magn. Res.* **1994**, *7*, 289.

(79) Mazzoni, M.; Conti, F.; Corvaja, C. *Appl. Magn. Reson.* **2000**, *18*, 351.

(80) Flamigni, L. *Pure Appl. Chem.* **2001**, *73*, 241.

(81) Schanze, K. S.; Walters, K. A. Photoinduced Electron Transfer in Metal-Organic Dyads. In *Organic and Inorganic Photochemistry*; Marcel Dekker: New York, 1998; Vol. 2: Molecular and Supramolecular Photochemistry; pp 75.

(82) Schuster, D. I.; Li, K.; Guldi, D. M. *C. R. Chimie* **2006**, *9*, 892.

(83) Rozenshtein, V.; Berg, A.; Levanon, H.; Krueger, U.; Stehlik, D.; Kandrashkin, Y.; van der Est, A. *Isr. J. Chem.* **2003**, *43*, 373.

(84) Yagi, M.; Kaneshima, T.; Torii, M.; Matsuo, K.; Higuchi, J. *Chem.Phys.Lett.* **1992**, *197*, 457.

(85) Megiatto, J. D. J.; Schuster, D. I.; de Miguel, G.; Wolfrum, S. *Angew. Chem. Int. Ed.* **2011**, *submitted*.

TOC

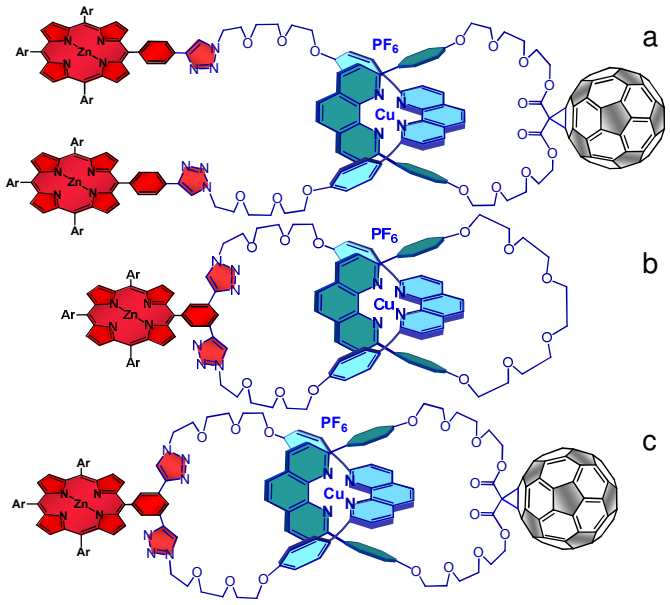

Figure 1.

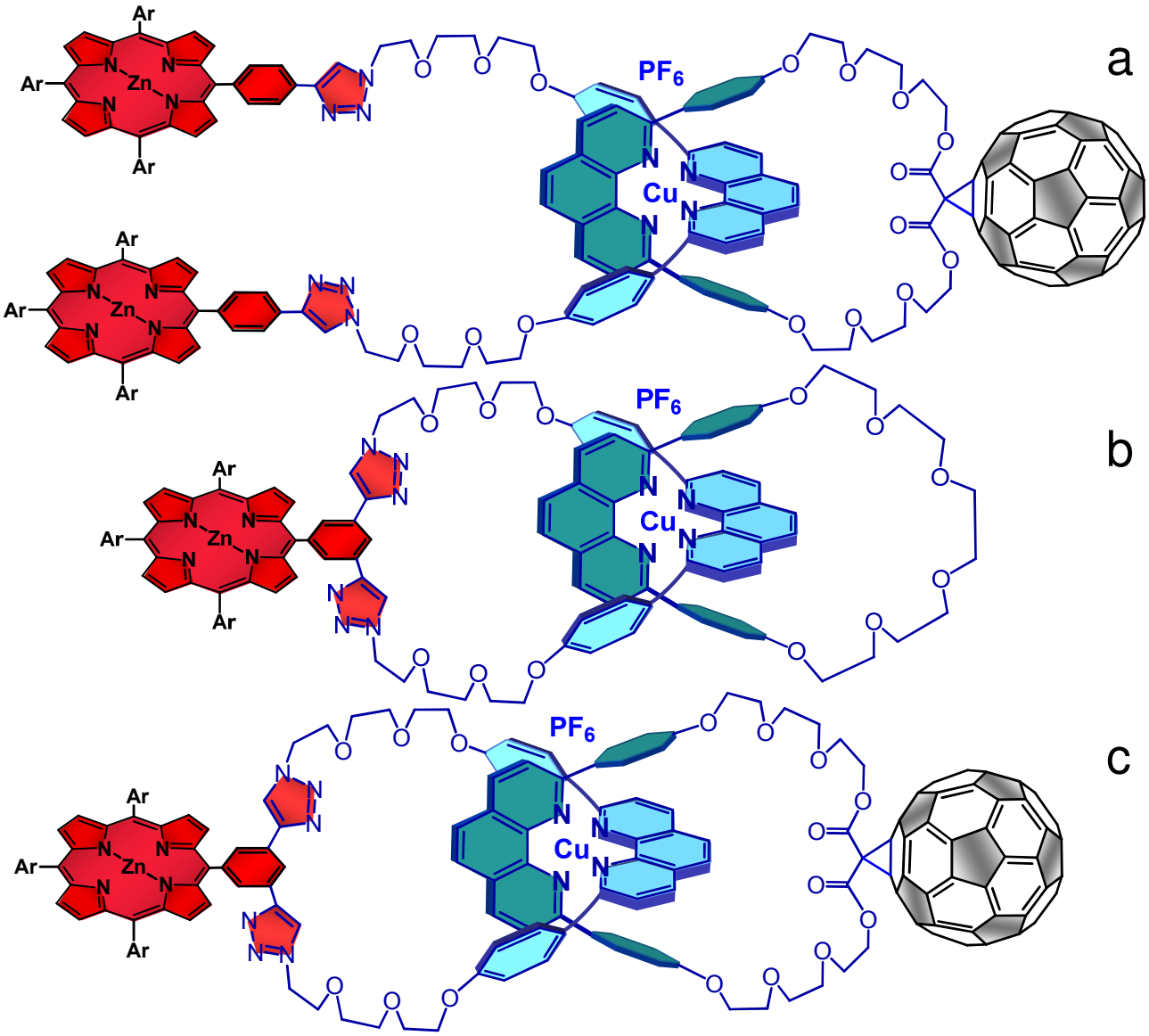

Figure 2.

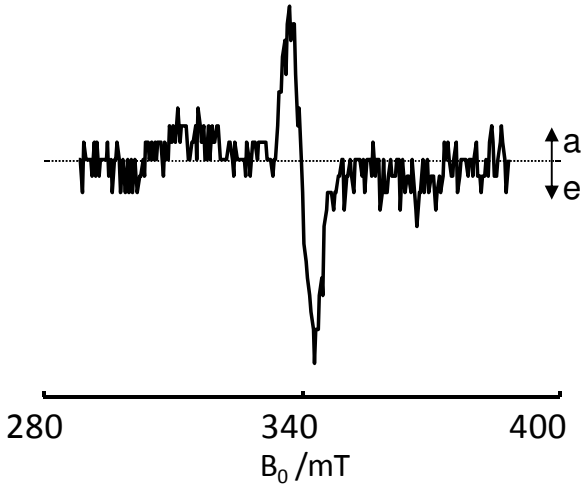

Figure 3.

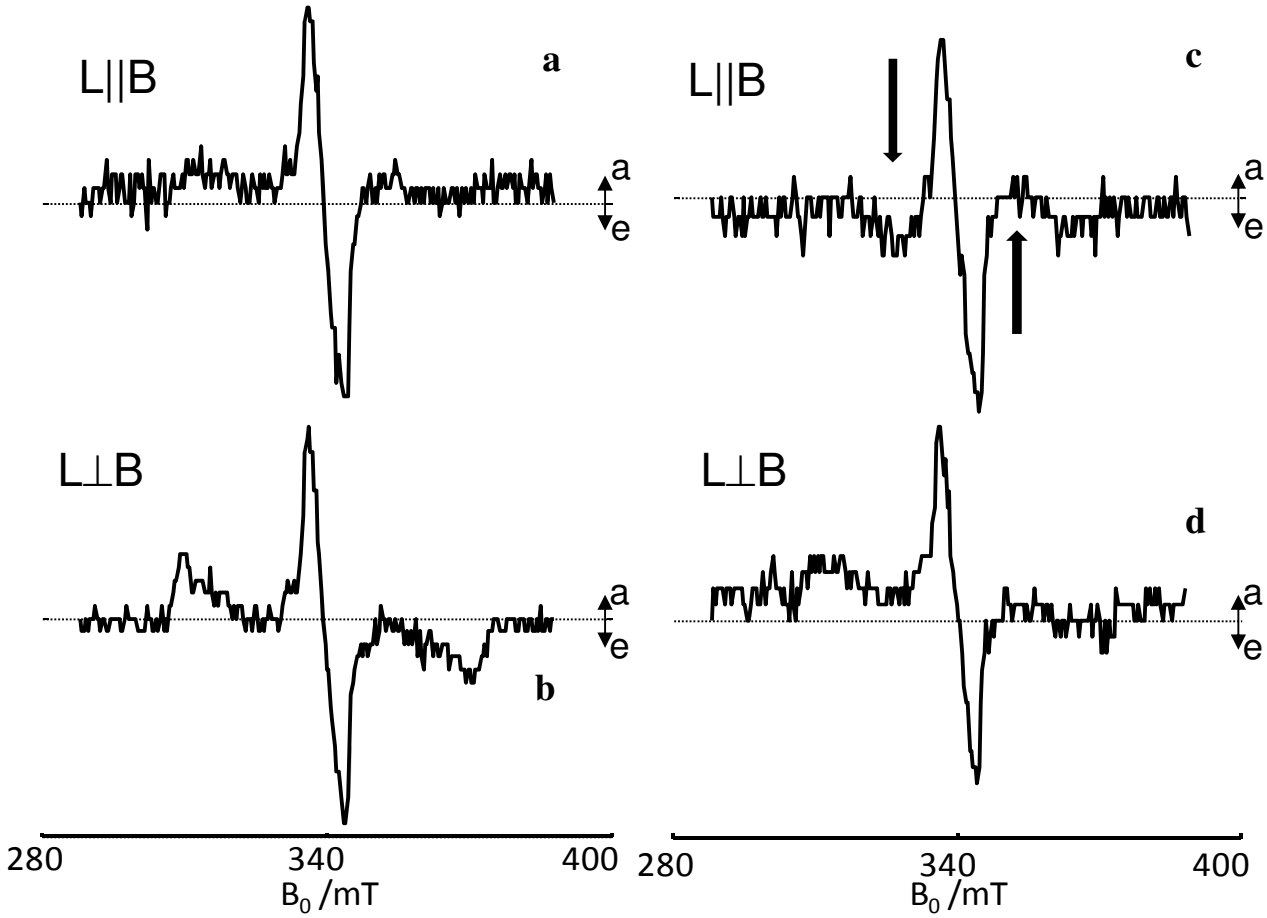

Figure 4.

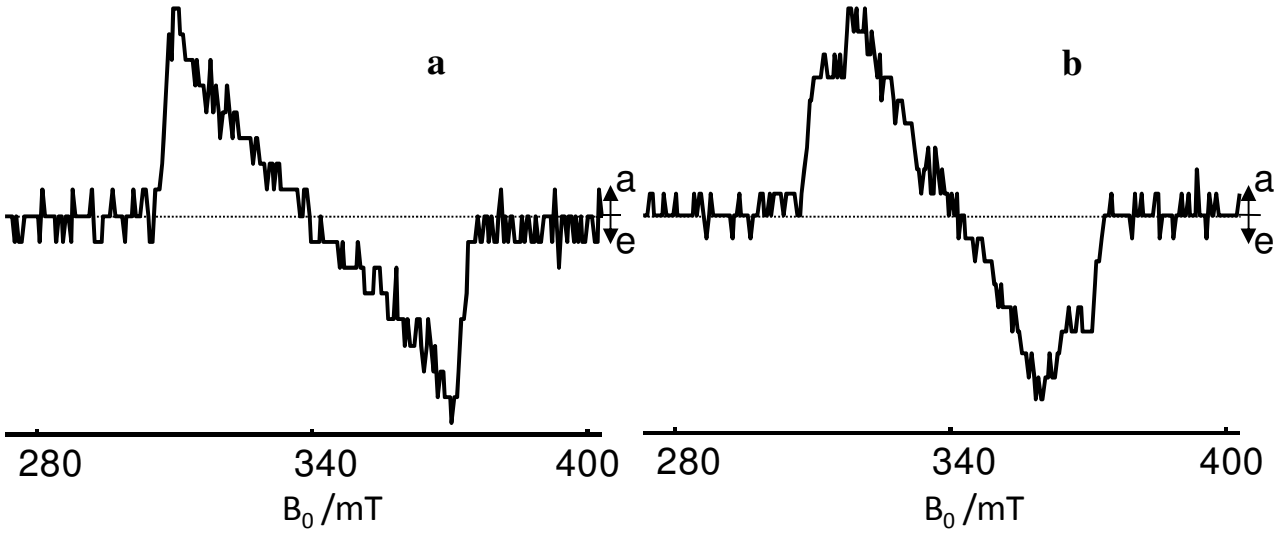

Figure 5.

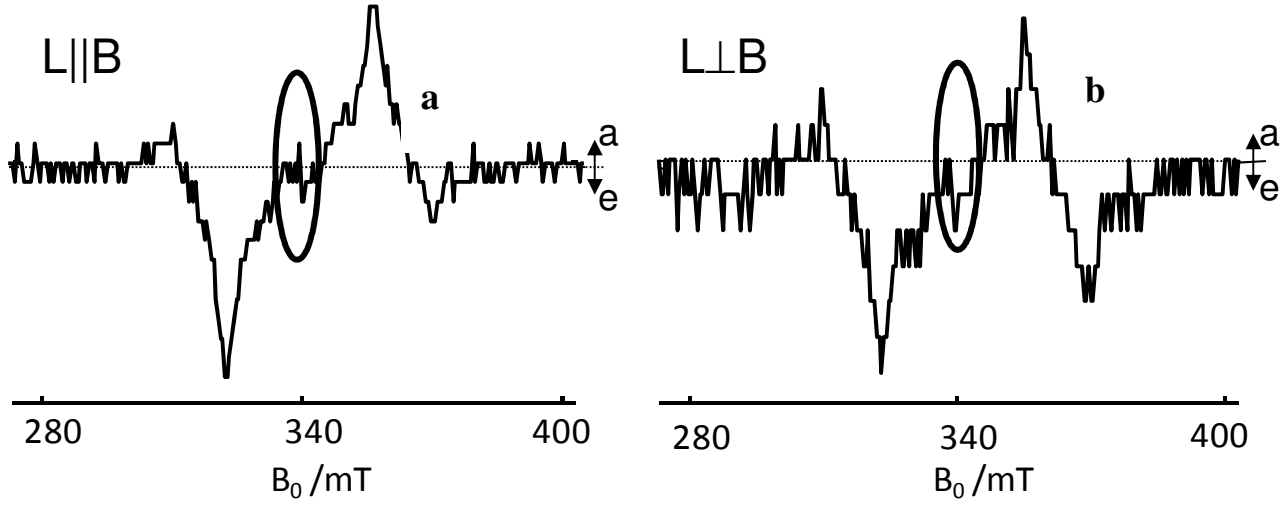

Figure 6.

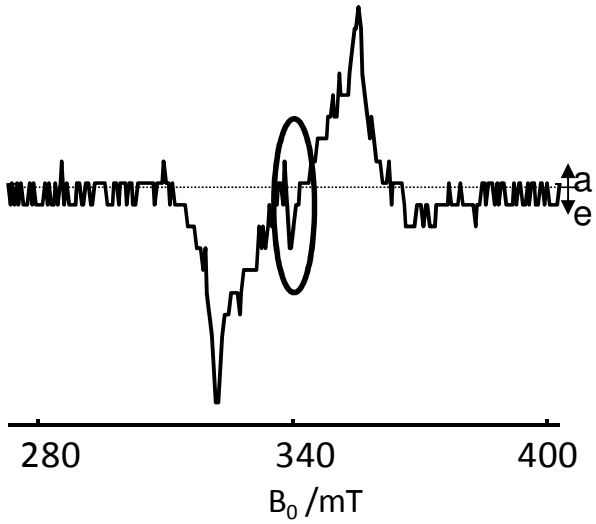

Figure 7.

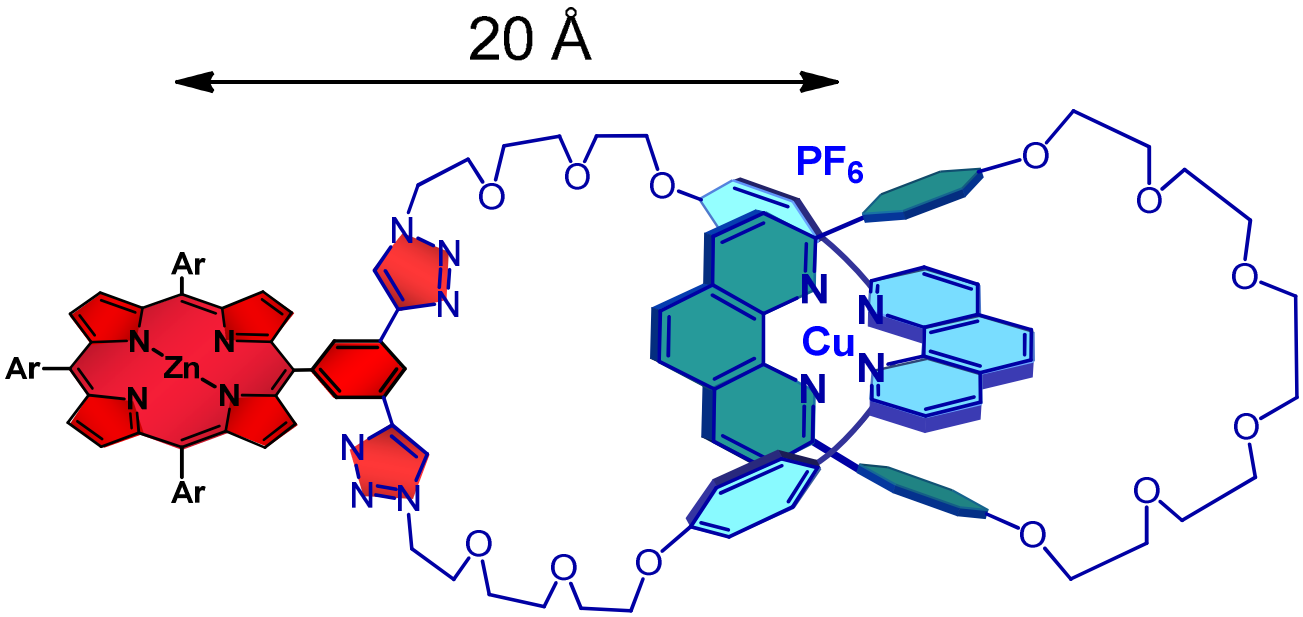

Figure 8.

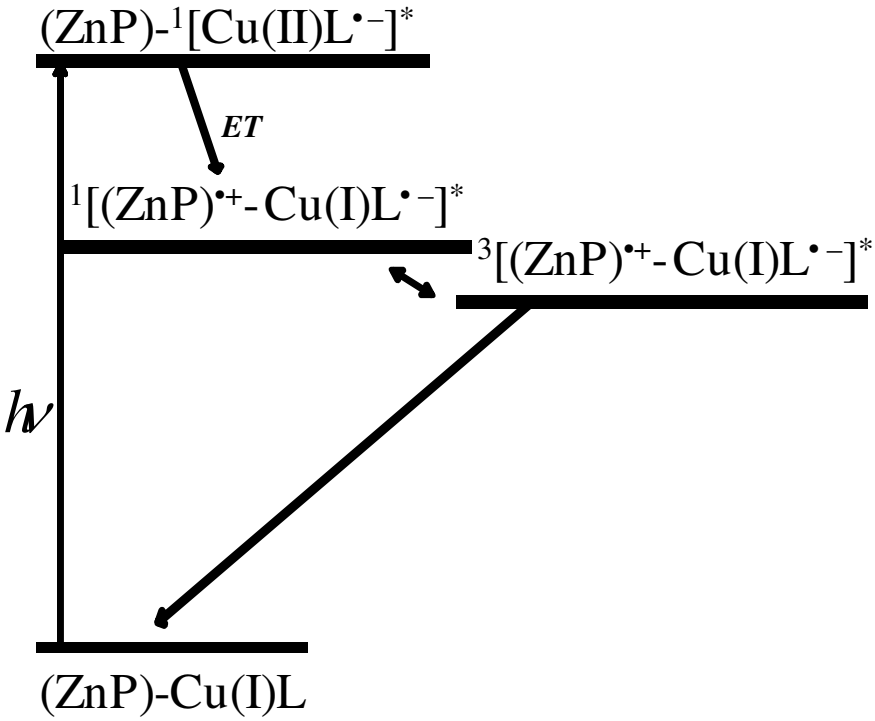

Figure 9.

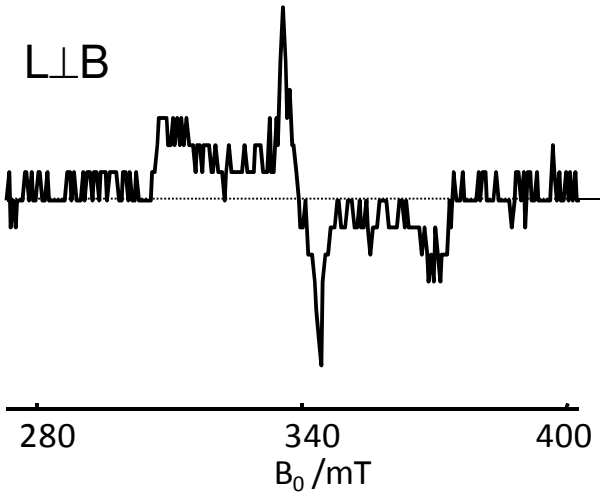

Figure 10.

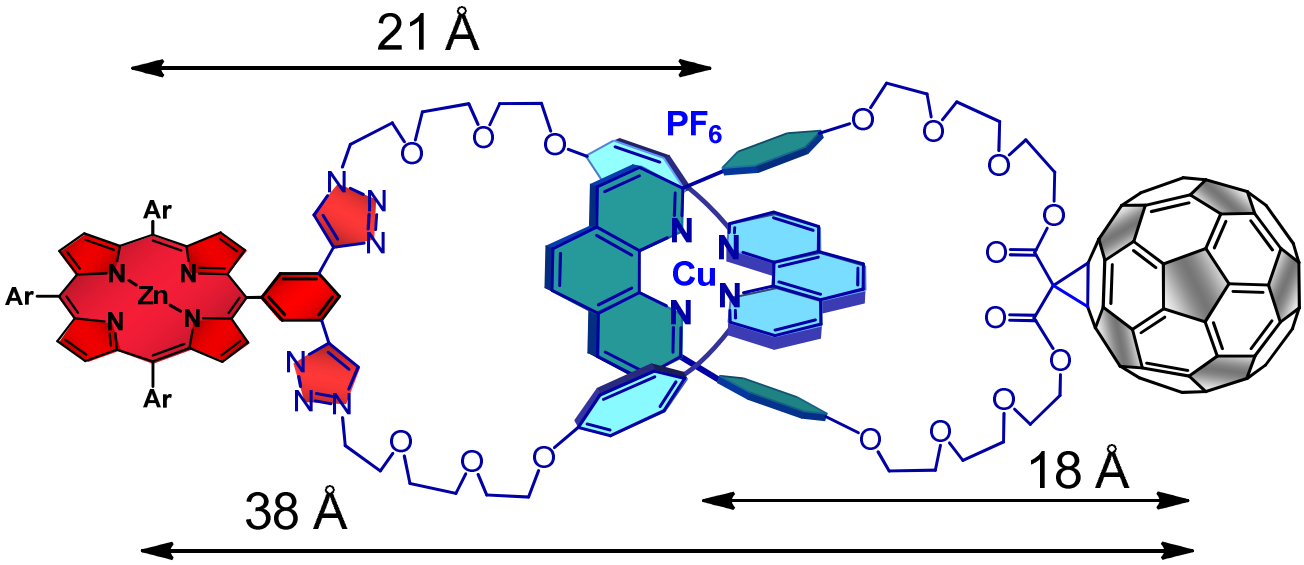

Figure 11.